CHAPTER III
POLYDIPHENYLAMINE/ZEOLITE Y COMPOSITES AND ELECTRICAL CONDUCTIVITY REPONSES TOWARD HALOGENATED HYDROCARBONS

3.1 Abstract

Composites of polydiphenylamine (PDPA) and zeolite Y with H^- as the cation (YH) was fabricated to be used as a sensing material towards non-halogenated and halogenated solvents (hexane, dichloromethane, 1, 2-dichloroethane, chloroform). These chemical are toxic towards human and environment and are widely used as solvents in various industries. PDPA, YH, and their composites were characterized by Fourier transform infrared spectroscopy, scanning electron microscopy, particle size analysis, surface area, and pore size analysis. The effects of the Si/Al ratio, zeolite content, and vapor concentrations were investigated. The electrical conductivity sensitivity of the composites towards the solvents was higher than the pristine doped polydiphenylamine (D-PDPA) by ~1 order of magnitude. The composites could discriminate a non-halogenated solvent from halogenated solvents. They possessed maximum electrical conductivity sensitivity values towards dichloromethane, but the composites did not respond to hexane. Generally, the sensitivity of the composites increased with increasing zeolite content and vapor concentration. The interactions between the composites and the vapors were investigated by FT-IR spectroscopy and UV-Vis spectroscopy. A mechanism for the interaction between the composites and the solvents was proposed.

Keywords: Conductive polymer; Electrical conductivity; Polydiphenylamine; Zeolite Y; Halogenated hydrocarbon

3.2 Introduction

Volatile organic compounds (VOCs) are organic compounds that easily evaporate at normal pressure and room temperature. The VOCs are widely used in daily products and used as solvents in various industries (Sidebottom and Franklin, 1996). Nevertheless, the toxicity of these chemical vapors causes serious environmental and human health concerns. The VOCs are divided into two groups; non-halogenated hydrocarbons, and halogenated hydrocarbons. Non-halogenated hydrocarbons are volatile hydrocarbons that do not contain a chlorine atom within the molecule. Normally, this group is found in daily life products such as plastics, cleaning solvents, and paints, and it can affect human health through the respiratory system. Examples of non-halogenated hydrocarbons are aliphatic hydrocarbons, aromatic hydrocarbons, alcohol, aldehyde, and ketones. The other type of VOCs is halogenated hydrocarbons which consist of a chlorine atom within the molecule. They are used in dry cleaning, metal cleaning, furniture making, thermoplastics production, degreasing, printing, paper and textile production, and paint removal (Sidebottom and Franklin, 1996). They are clear liquids, and vaporize at room temperature (Penza and Cassano, 2003; Kukla et al., 2009; Feng and MacDiarmid, 1999). Examples of halogenated solvents are trichloroethylene, perchloroethylene, methylene chloride, ethylene chloride, carbon tetrachloride, chloroform, and methyl chloroform. The toxicity of these chemical vapors is more severe to human health than non-halogenated hydrocarbons. The solvents pose a major source of environmental problems such as stratospheric ozone depletion, smog formation, acid rain production, and global warming. Health problems caused by exposing humans to these solvents are systemic, immunological, neurological, reproductive, developmental, and genotoxic and carcinogenic in nature; which can lead to death (Whitaker and Jones, 1965). The severity of the chemicals on human health depends on the concentration and exposure levels. The National Institute of Occupational Safety and Health (NIOSH) defined the limit for personal exposure to the chemical that cause to death or immediate or delayed permanent adverse health effects as the immediately dangerous to life or health concentrations (IDLHs) (NOOA, 2013). For instance, the exposure level of chloroform that leads to death in humans is ~40,000

ppm (Featherstone, 1947). The level of chloroform that leads to human loss of responsiveness, loss of skeleton muscle reflex, and decreased stress response is less than 22,500 ppm (Whitaker and Jones, 1965; Anesthesia, 2013). The deadly inhalation concentration for methylene chloride, or dichloromethane (DCM), in a study of animals, was ~3,000 ppm (Williams et al., 2000). Hence, effective sensory systems are required to identify the presence of these solvents. One development of sensing materials has focused on conductive polymers due to their unique properties. They are: light weight, easy to synthesize, possess high sensitivity and short response time, and have good mechanical properties over metal oxides (Bailey et al., 2008; Bai and Shi, 2007; Albert et al., 2000). Polydiphenylamine (PDPA) is an N-aryl substituted derivative of polyaniline and it shows better mechanical strength, electrochemical, conductivity, and electro chromic properties than polyaniline (Li et al., 2007; Hua and Ruckenstein, 2003, 2005; Chung et al., 2001);. Additionally, PDPA has been used as a sensing material for many sensory systems: pH sensors, CO sensors, and glucose biosensors (Santhosh et al., 2007, 2009; Rodríguez et al., 2007). Another group of materials that can also be used as sensing materials are zeolites. Zeolites are aluminosilicate minerals that have micro porous cages within their crystal structures. Due to their unique structures, zeolites can act as molecular sieves to separate different types of molecules. Thus, zeolites can be used as a catalyst support, an absorbent for moisture and toxic gases, and for ion exchange. Recently, there have been several studies on conductive polymer/zeolite composites as gas or vapor sensing materials (Hugon et al., 2000; Wu et al., 2009; Xu et al., 2006).

This work is aimed at fabricating the composites between D-PDPA and zeolite Y with H⁻ as a cation (YH) to discriminate between the non-halogenated and halogenated hydrocarbon solvents, based on the electrical conductivity response when exposed to halogenated vapors. The influences of the Si/Al ratio, YH content, and vapor concentration of the halogenated solvents—dichloromethane (DCM), 1,2-dichloroethane (DCE), and chloroform—on the electrical conductivity response of D-PDPA/zeolite Y composites (D-PDPA/YH) are investigated. The physical adsorption of the halogenated solvents on the composites is examined by FT-IR and UV-Vis spectroscopy.

3.3 Experimental

3.3.1 Materials

Diphenylamine, DPA (reagent, Sigma Aldrich), ammonium persulfate, $(NH_4)_2S_2O_8$, (AR grade, Riedel-deHaën), and 37 %v/v of hydrochloric acid, HCl (ACS reagent, J T Baker), were used at a mole ratio of 100:1 ($N_{HCl}/N_{monomer}$). Zeolite Y (Zeolite International) with H^- as a cation (YH), having Si/Al ratios of 5.1 (YH[5.1]), 30 (YH[30]), 60 (YH[60]), and 80 (YH[80]) were used in powder form. Ammonium hydroxide, NH_4OH (AR grade, Panreac), toluene (AR grade, Panreac), isopropyl alcohol (AR grade, Burdick & Jackson), and ethanol (AR grade, Lab Scan) were used without further purification.

3.3.2 Chemical Vapor Detection

Dichloromethane, DCM (AR grade, Lab Scan), 1,2-dichloroethane, DCE (AR grade, Lab Scan), chloroform (AR grade, Lab Scan), and hexane (AR grade, Lab Scan) were used as the chemical vapors in this work.

3.3.3 Synthesis of PDPA and Doping Process

Polydiphenylamine (PDPA) was synthesized via chemical oxidative polymerization (Orlov *et al.*, 2006; Sathiyanarayanan *et al.*, 2006). A DPA solution in toluene was mixed with $(NH_4)_2S_2O_8$ solution in distilled water. The solution mixture was stirred by using an overhead stirrer, cooled to 0 °C for 15 minutes, and then a HCl solution in distilled water was added to the mixture. The reaction mixture was continuously stirred at 0 °C for 4 hrs; next the green slurry of PDPA was precipitated. The precipitate was washed with isopropyl alcohol at least 3 times. Then the HCl-doped PDPA was de-doped in a mixture of ethanol and ammonium hydroxide solution (1:4 v/v) for 24 hrs. The neutralized PDPA was doped with 5M HCl solution at a mole ratio of 100:1 ($N_{HCl}/N_{monomer}$) and stirred at room temperature for 24 hrs. The resultant doped PDPA, D-PDPA, was filtered and dried in a vacuum oven at room temperature for 24 hrs to remove excess HCl.

3.3.4 Preparation of D-PDPA Pellets and D-PDPA/YH Composites

The D-PDPA powder was ground with the YH powder at various YH concentrations (0, 5, 10, 20, and 30 %v/v). The D-PDPA powder and D-PDPA/YH composites were compressed into pellets for the electrical conductivity and sensitivity measurements with a hydraulic press machine (GRASEBY SPECAC) under a 4-5 ton load. Pellets were produced in disc form using a 1 cm stainless steel die. The thickness of each pellet was between 0.03-0.04 cm as measured by a digital thickness gauge (PEAACOCK, dial stand type model PDN-20).

3.3.5 Characterization

Fourier transform infrared (FT-IR) spectra of D-PDPA were recorded with a Thermo Nicolet, Nexus 670 FT-IR spectrometer using a resolution of 2 cm^{-1}, a scan number of 32, and a wavenumber range of 400-4000 cm^{-1}. Scanning electron micrographs of D-PDPA, YH, and D-PDPA/YH were taken using a HITACHI, S-4800 scanning electron microscope (SEM) with a magnification of 10,000x, operating at 10 kV. The particle sizes of D-PDPA and YH were measured by using a Mastersizer X particle size analyzer. The surface area and pore size of YH were measured with a Physisorption, Quantachrome, Autosorb- 1MP surface area analyzer. Zeolite powder was weighed and out gassed at 300 °C over night before adsorption and desorption with He and N_2 gases. During the operation, the zeolite powder was cooled by liquid N_2. The specific density of the D-PDPA and YH were measured with a pycnometer. The optical properties of the D-PDPA and YH when exposed to DCM were taken by a UV-Vis spectrophotometer (SHIMADZU, UV 1800) in the wavelength number of 200 nm to 500 nm at room temperature.

3.3.6 Conductivity and Sensitivity Measurements

The conductivity and the sensitivity of D-PDPA, YH, and D-PDPA/YH towards halogenated solvents were measured by a custom built two-point probe connected with a conductivity meter (KEITHLEY 6517A) which applied voltage: the resultant current was measured. The electrical conductivity was calculated by the equation $\sigma = (I/KVt)$, where I is the measured current (A), V is the applied voltage (V), t is the thickness (cm), and K is the geometric correction factor

of the two-point probe as calibrated by standard silicon wafer sheets with known specific resistivity values. All measurements were taken at 27 ± 1 °C and at atmospheric pressure. The electrical conductivity responses and sensitivities under exposure to air, N_2, and halogenated solvents were determined by the equation $\Delta\sigma = \sigma_{halogenated\ solvents} - \sigma_{N2}$, initial and $\Delta\sigma/\sigma_{N2}$, initial, respectively, where $\Delta\sigma$ is the difference in the specific electrical conductivity (S/cm), σ_{N2}, initial is the specific electrical conductivity in N_2 before exposure (S/cm), and $\sigma_{halogenated\ solvent}$ is the specific electrical conductivity (S/cm) under halogenated solvent exposure. The effect of the halogenated solvent concentration was determined at concentrations of 5, 10, 15, 20, 25, 30, 35, and 50 %v/v in N_2.

3.4 Results and Discussion

3.4.1 Characterization of D-PDPA and YH

The FT-IR spectra of D-PDPA showed absorption peaks at 3388, 3053, 1594, 1505, 1318, 1173, 821, 748, and 748-694 cm^{-1}. These peaks can be assigned to: N-H stretching, C-H in the aromatic ring, quinoid ring stretching, phenyl hydrogen, benzenoid ring stretching, vibration band of N_2 in quinone, C-H out of plane aromatic, 1, 4 substituted on aromatic rings, and C-H out of plane bending vibration, respectively (Hua and Ruckenstein, 2003; Sathiyanarayanan et al., 2006; Athawale et al., 1999; Santana and Dias, 2003). The FT-IR spectra of YH show major absorption peaks at 1213, 1080, 836, and 459 cm^{-1}. These peaks can be assigned to the asymmetric stretch of the internal tetrahedral, the asymmetric stretch of the external linkage, the symmetric stretch of the external linkage, and the T-O bend of the internal tetrahedral, respectively (George and Christidis, 2008; Kondru et al., 2008). The average particle size of D-PDPA and YH was 125.96 ± 5.51 µm and 20.66 ± 0.58 µm, respectively. The surface area, pore size, and pore volume of YH are comparable at various Si/Al ratios (Table 3.1). The specific density of D-PDPA and YH is 0.85 ± 0.01 g/cm^3 and 1.61 ± 0.35 g/cm^3, respectively. The micrographs shown in Figure 3.1 reveal that the shapes of YH are square shaped (Figure 3.1a) and

the shape of the D-PDPA particles (Figure 3.1b) is irregular. Nevertheless, the YH particles are dispersed uniformly within the D-PDPA matrix (Figure 3.1c).

3.4.2 Sensitivity of D-PDPA and YH towards Halogenated Solvents

The electrical conductivity sensitivity of D-PDPA, YH towards the four solvents is shown in Figure 3.2. The D-PDPA and YH exhibit negative responses towards all four solvents. Table 3.2 shows the initial electrical conductivity values of D-PDPA, YH, D-PDPA/YH[80] when exposed to halogenated solvents. The sensitivity values of D-PDPA, YH towards the four solvents, shown in Table 3.3, show that D-PDPA and YH possess maximum sensitivity responses towards DCM followed by DCE and chloroform, but they hardly respond to hexane. This is presumably due to the differences in the molecular structure, the strength of the electrostatic interaction, the dipole moment, and the dielectric constant (Archer $et\ al.$, 2005) (Table 3.4). The interaction between D-PDPA and the vapors occurs at the N-H^+ site and the Cl^- atom. Since, the dipole moment of DCM (1.80) is higher than that of DCE (1.60) and chloroform (1.10), the dipole-dipole interaction between the Cl^- atom of the DCM molecule and the N-H^+ site of D-PDPA is stronger than those of DCE and chloroform (Smallwood, 1996). Therefore, the sensitivity of D-PDPA toward DCM is higher than those of other vapors. Because the hexane structure is an aliphatic hydrocarbon chain and it has no dipole moment, the interaction between D-PDPA and hexane vapor is suspected to be physical adsorption on the matrix surface without the dipole-dipole interaction, unlike the other chlorinated hydrocarbon molecules (Lu $et\ al.$, 2009; Xu $et\ al.$, 2002; Jose $et\ al.$, 2004). Therefore, the sensitivity of D-PDPA towards hexane is low. For zeolite, the interaction between YH and the vapors is the hydrogen bonding at the Si-O^- or Al-O^- site and the –H atom of the vapor molecules. The sensitivity of YH towards DCM is also higher than those of DCE (~50%) and chloroform (~60%). For DCM, there are two hydrogen atoms that form the hydrogen bond with D-PDPA and YH. For DCE, a lower sensitivity than DCM occurs due to the larger chemical structure of DCE over DCM, known as the steric effect. For chloroform, since there is only one hydrogen atom in the chemical structure, and the dipole moment and dielectric constant are also very low, the strength of the hydrogen bonding between YH and chloroform is lower than

the strength of the hydrogen bonding between YH and DCM and YH and DCE (Smallwood, 1996). Moreover, the sensitivity of YH increases with increasing Si/Al ratio. This occurs because the hydrophobicity of zeolite increases with the Si/Al ratio (Auerbach et al., 2003). Hence, the halogenated solvents, which are non-polar solvents, produce more favorable responses towards the zeolites YH with higher Si/Al ratios. Therefore, the YH[80] was chosen to form composites with D-PDPA, in order to further improve the sensitivity of D-PDPA towards the halogenated solvents.

3.4.3 Sensitivity of D-PDPA/YH[80] Composites toward Halogenated Solvents: Effect of Zeolite Y Contents

The effect of YH[80] content on the sensitivity of D-PDPA/YH[80] towards the halogenated solvents was investigated. The composites show negative sensitivity towards the solvents (Table 3.3). According to the doping theory (Freund and Deore, 2007), D-PDPA is doped via the p type doping process. When it is exposed to the vapors, which are electron-donating groups, the vapors will give up an electron to fill the hole on the D-PDPA backbone. Thus, the electron mobility along the D-PDPA backbone is more difficult, resulting in a decrease in conductivity, which is why the composites show negative sensitivity towards the solvents. It appears that the sensitivities of the composites are higher than those of pure D-PDPA by about 1 order of magnitude towards DCM and DCE; the sensitivity increases with increasing YH[80] content (Figure 3.3). With a higher zeolite content, a greater interaction results between the micro-porous structure and the target vapor. With a YH[80] content of ~30 %v/v, the composite shows the highest sensitivity. The sensitivity of chloroform is quite constant with respect to the YH[80] content because it has no dipole moment and very low dielectric constants (Ayad et al., 2008). The composite does not respond to hexane, even when the zeolite content increases to 30 %v/v, because the interaction between the composite and hexane is only physical absorption. The sensitivity of the composite towards the three halogenated solvents is in this order: DCM>DCE>chloroform. Therefore, it can be concluded that the addition of zeolites can improve the sensitivity of D-PDPA and it can discriminate a nonhalogenated solvent from halogenated solvents.

3.4.4 Sensitivity of D-PDPA/YH[80] Composites toward Halogenated Solvents: Effect of Vapor Concentration

The composite consisting of 30 %v/v of YH[80] with D-PDPA (D-PDPA/30% YH[80]) was next investigated with respect to DCM and DCE at various vapor concentrations. The sensitivity of the composite. which is exposed to DCM. increases from $(-1.23 \pm 0.004) \times 10^{-2}$ to $(-3.47 \pm 1.64) \cdot 10^{-1}$ as the vapor concentration increases from 7.696 ppm to 153.914 ppm. respectively (Figure 3.4). When the composite is exposed to DCE. the sensitivity increases from $(-1.09 \pm 0.96) \times 10^{-1}$ to $(-1.77 \pm 0.04) \times 10^{-1}$ as the vapor concentration increases from 1.015 ppm to 20.299 ppm. respectively. When the composites are exposed to both of DCM and DCE. they exhibit linear relationships between the sensitivity and vapor concentration. As the vapor concentration increases. the sensitivity of D-PDPA/30% YH[80] increases. A similar result has been also found by Jiang *et al.* (2003). They prepared a polypyrrole and polyvinylalcohol composite via in situ vapor state polymerization to detect methanol vapors. The composite showed a linear relationship between sensitivity. The limit of detectin of DCM and DCE that the composite can detect are 1.930 ppm and 449 ppm. respectively: these values are equivalent to the IDLHs value (Smallwood. 1996: Tukker and Simons. 1999: Satcher. 1994). The chemical interactions between DCM and the composites were investigated by FT-IR spectroscopy and UV-VIS spectroscopy. Figure 3.5 shows the FT-IR spectra of the vapors. Before exposure to DCM. the absorption peaks at 1594. 1505. 1318. 1213. 1080. 836. and 748 cm^{-1} can be assigned to the quinoid ring stretching of D-PDPA (Athawale *et al..* 1999), the phenyl hydrogen of D-PDPA (Hua and Ruckenstein, 2003). the benzenoid ring stretching of D-PDPA. the asymmetric stretch of the internal tetrahedral in YH[80]. the asymmetric stretch of the external linkage. the symmetric stretch of external linkage (George and Christidis. 2008: Kondru *et al..* 2009). and the 1. 4 substituted on aromatic rings (Sathiyanarayanan *et al..* 2006). respectively. During exposure to DCM. new peaks occur at 3097. 1285. and 752 cm^{-1} which can be assigned to the hydrogen bonding between the oxygen atom of YH and the hydrogen atom of DCM molecule (Silverstein *et al..* 2005). CH_2 in CH_2-Cl_2 (Lambert *et al..* 2010), and the interaction

of the chlorine atom of DCM and the nitrogen atom of D-PDPA backbone (Martin *et al.*, 1997), respectively. After exposure to DCM, the peaks at 3097, 1285, and 752 cm^{-1} disappear. This indicates that no interaction occurs between the composite and DCM molecules. The proposed mechanism is shown in Figure 3.6. From the proposed mechanism, the FT-IR absorption band of D-PDPA cannot be clearly discerned when exposed to DCM, thus the second derivative of the spectrum is used instead. During exposure to DCM, the absorption bands at 1596 and 1318 cm^{-1} corresponding to the quinoid ring stretching and the benzenoid ring stretching, respectively shift from the original positions before exposed to DCM by 4 cm^{-1} for the quinoid ring stretching and by 7 cm^{-1} for the benzenoid ring stretching as shown in Figure 3.7. Anitha and Subramanian (2004) have also observed that the FT-IR absorption band of polyaniline when exposed to DCM shifted by 3 cm^{-1} due to the electron displacement from chlorine atom of DCM to the polyaniline backbone.

The UV-Vis spectra are used to confirm the interaction between DCM and the composite. The spectrum of the D-PDPA is shown in Figure 3.8a. There are two absorption bands, one at 282 nm which corresponds to the characteristic absorption bands of DCM, and the other at 342 nm which corresponds to the n-π* transition at $-N^-=$ of the D-PDPA backbone (Vivekanandan *et al.*, 2011). It is clear from Figure 3.8a that the absorption band is blue shifted from 342 nm to 334 nm and the absorbance intensity decreases with increasing DCM concentration from 5%v/v to 25 %v/v. This indicates that the shift in the absorption band is due to DCM giving up an electron to fill hole on D-PDPA backbone. Thus, the electron mobility along the D-PDPA backbone becomes more difficult, and the band gap of D-PDPA increases. It needs more energy to accelerate the electron to a higher conduction band, resulting in the shift of the electronic band of D-PDPA to a higher energy or a lower wavelength (Chung *et al.*, 2001; Santana and Temperini, 1996). The absorption band observed at 271 nm corresponds to the $-Si-O_4^{2-}$ site on the YH framework (Bennur *et al.*, 2004) (Figure 3.8b). The absorption band is red shifted from 271 nm to 277 nm and the absorbance intensity decreases with increasing DCM concentration from 5 %v/v to 25 %v/v because the electron donor and acceptor interact between the $-Si-O_4^{2-}$ site of the YH framework and the –H atom of the DCM

molecule. For D-PDPA/30% YH[80] composite (Figure 3.8c), they are also two absorption bands at ~340 nm and ~265 nm which correspond to the n-π* transition at $-N^+=$ of the D-PDPA backbone and the $-Si-O_4^{2-}$ site on the YH framework, respectively. The absorption band at 342 nm is blue shifted from 340 nm to 336 nm. The absorption band at 262 nm is red shifted to 275 nm. This occurs similarly to D-PDPA and YH[80]. It can be concluded that the interaction between the composite of D-PDPA/30% YH[80] and DCM occurs as shown in the proposed mechanism (Figure 3.6). Choi et al. (1996) studied iodine absorption on various zeolites. The absorption band was gradually red shifted when the iodine molecules increasingly absorbed on the zeolite Y framework. They attributed the phenomenon to $-Si-O_4^{2-}$ donating an electron to the adsorbed iodine molecules.

3.4.5 The Temporal Response D-PDPA/YH[80] Composites

The induction time of the D-PDPA when exposed to DCM, DCE, and chloroform was around 13.50 ± 2.12, 8.56 ± 1.25, 15.00 ± 1.41 min, respectively. For the D-PDPA/30% YH[80] composite, the induction time was about 18.50 ± 0.71 min for DCM, 17.65 ± 0.43 min for DCE, 15.95 ± 1.34 min for chloroform. The results showed that the induction time of the composite was higher than D-PDPA. This suggests that the presence of zeolite, a micro porous structure, introduces more active sites for the vapors to absorb. D-PDPA showed a reduction time when exposed to DCM, DCE, and chloroform of 9.50 ± 4.86, 6.35 ± 1.57, and 13.75 ± 7.84 min, respectively. The reduction times of the composite when exposed to DCM, DCE, and chloroform were 6.00 ± 3.04, 6.10 ± 0.49, and 7.05 ± 2.87 min, respectively. The reduction time of the D-PDPA/30% YH[80] composite was also higher than the D-PDPA due to the micro porous structure of the zeolite. A similar result was also found by Thuwachaowsoan et al. (2007). They fabricated a composites of poly(3-thiopheneacetic acid) (Pth) with zeolites L, mordenite (MOR), and beta (BETA) as H_2 gas sensors. They found that the induction time of the Pth 200:1/BETA was longer than that of the polymer and other composites. They concluded that the presence of zeolite introduces more reactive sites to interact with the H_2 molecules.

3.5 Conclusions

D-PDPA was fabricated into a composite with YH to detect the toxic halogenated solvent vapors DCM, DCE, chloroform, and hexane. The composites show improved sensitivity responses towards DCM, DCE, and chloroform than hexane, because of the differences in the chemical structures of the dipole moment, and the dielectric constants of the target vapors. The sensitivities of the composites increase with increasing Si/Al ratio, zeolite content, and vapor concentration due to greater interactions between the zeolite and target vapors. For the temporal response, the induction and recovery times of the composite were higher than those of the pristine D-PDPA due to more active sites being available for the vapor molecules. The UV-Vis spectra show that the interaction between the composite and DCM does exist: the UV absorption band of D-PDPA and YH is shifted by the delocalization of the Cl^- atom. The electron donor, acceptor interaction occurs between YH and the $-$H atom when exposed to DCM. It may be concluded that the fabricated composites possess a potential use as a sensing material for discriminating non-halogenated solvents from halogenated hydrocarbon solvents.

3.6 Acknowledgments

3.7 References

Albert, K.J., Lewis, N.S., Schauer, C.L., Sotzing, G.A., Stitzel, S.E., Vaid, T.P., and Walt, D.R. (2000) Cross-reactive chemical sensor arrays. Chemical Reviews. 100(7), 2595-2626.

Anitha, G. and Subramanian, E. (2003) Dopant induced specificity in sensor behaviour of conducting polyaniline materials with organic solvents. Sensors and Actuators B: Chemical. 92(1–2), 49-59.

Archer, M., Christophersen, M., and Fauchet, P.M. (2005) Electrical porous silicon chemical sensor for detection of organic solvents. Sensors and Actuators B: Chemical. 106(1), 347-357.

Athawale, A.A., Deore, B.A., and Chabukswar, V.V. (1999) Studies on poly(diphenylamine) synthesized electrochemically in nonaqueous media. Materials Chemistry and Physics. 58(1), 94-100.

Auerbach, S.M., Carrado, K.A., and Dutta, P.K. (Eds.) (2003) Handbook of Zeolite Science and Technology. New York: Marcel Dekker.

Ayad, M.M., El-Hefnawey, G., and Torad, N.L. (2008) Quartz crystal microbalance sensor coated with polyaniline emeraldine base for determination of chlorinated aliphatic hydrocarbons. Sensors and Actuators B: Chemical. 134(2), 887-894.

Bai, H. and Shi, G. (2007) Gas sensors based on conducting polymers. Sensors. 7(3), 267-307.

Bailey, A.L.P.S., Pisanelli, A.M., and Persaud, K.C. (2008) Development of conducting polymer sensor arrays for wound monitoring. Sensors and Actuators B: Chemical. 131(1), 5-9.

Bennur, T.H., Srinivas, D., and Sivasanker, S. (2004) Oxidation of ethylbenzene over "neat" and zeolite-Y-encapsulated copper tri- and tetraaza macrocyclic complexes. Journal of Molecular Catalysis A: Chemical. 207(2), 163-171.

Choi, S.Y., Park, Y.S., Hong, S.B., and Yoon, K.B. (1996) Iodine as a visible probe for the evaluation of zeolite donor strength. Journal of the American Chemical Society. 118(39), 9377-9386.

Chung, C.Y., Wen, T.C., and Gopalan, A. (2001) Identification of electrochromic sites in poly(diphenylamine) using a novel absorbance-potential-wavelength profile. Electrochimica Acta. 47(3). 423-431.

contributors, W. "Anesthesia " Wikipedia. 28 Sep 2012. 9 Oct 2012 <http://en.wikipedia.org/w/index.php?title=Anesthesia&oldid=515002047>

De Santana, H. and Dias, F.C. (2003) Characterization and properties of polydiphenylamine electrochemically modified by iodide species. Materials Chemistry and Physics. 82(3). 882-886.

Featherstone, H.W. (1947) Chloroform. Anesthesiology. 8(4). 362-371.

Feng, J. and MacDiarmid, A.G. (1999) Sensors using octaaniline for volatile organic compounds. Synthetic Metals. 102(1–3). 1304-1305.

Freund, M.S. and Deore, B. (2007) Self-Doped Conducting Polymers. New York: John Wiley.

George E. and Christidis, H.P. (2008) Synthesis of FAU type zeolite Y from natural raw materials: hydrothermal SiO_2 sinter and perlite glass. The Open Mineralogy Journal. 2(1). 1-5.

Hua, F. and Ruckenstein, E. (2003) Water-soluble conducting poly(ethylene oxide)-grafted polydiphenylamine synthesis through a "Graft Onto" process. Macromolecules. 36(26). 9971-9978.

Hua, F. and Ruckenstein, E. (2005) Hyperbranched sulfonated polydiphenylamine as a novel self-doped conducting polymer and its pH response. Macromolecules. 38(3). 888-898.

Hugon, O., Sauvan, M., Benech, P., Pijolat, C., and Lefebvre, F. (2000) Gas separation with a zeolite filter, application to the selectivity enhancement of chemical sensors. Sensors and Actuators B: Chemical. 67(3). 235-243.

Jiang, L., Jun, H.K., Hoh, Y.S., Lim, J.O., Lee, D.D., and Huh, J.S. (2005) Sensing characteristics of polypyrrole–poly(vinyl alcohol) methanol sensors prepared by in situ vapor state polymerization. Sensors and Actuators B: Chemical. 105(2). 132-137.

Jose, K.A., Biju, P., Ashwin, W., Vijay, K.V., and Reddy, C.C. (2004) A compact wireless gas sensor using a carbon nanotube/PMMA thin film chemiresistor. Smart Materials and Structures. 13(5). 1045.

Kondru, A.K., Pradeep, K., and Shri, C. (2009) Catalytic wet peroxide oxidation of azo dye (Congo red) using modified Y zeolite as catalyst. Journal of Hazardous Materials. 166(1), 342-347.

Kukla, A.L., Pavluchenko, A.S., Shirshov, Y.M., Konoshchuk, N.V., and Posudievsky, O.Y. (2009) Application of sensor arrays based on thin films of conducting polymers for chemical recognition of volatile organic solvents. Sensors and Actuators B: Chemical. 135(2), 541-551.

Lambert, J.B., Gronert, S., Shurvell, H.F., and Lightner, D. (2010) Organic Structural Spectroscopy. New Jersey: Prentice Hall PTR.

Li, C.Y., Wen, T.C., Guo, T.F., and Hou, S.S. (2008) A facile synthesis of sulfonated poly(diphenylamine) and the application as a novel hole injection layer in polymer light emitting diodes. Polymer. 49(4), 957-964.

Liang, L., Guangzhong, X., Yadong, J., Xiaosong, D., and Ping, S. (2009, October) Organic vapor adsorption behavior of poly (3-henxylthiophene) films on quartz crystal microbalance. Paper presented at 2009 International Conference on Optical Instruments and Technology: Advanced Sensor Technologies and Applications. Shanghai, China.

Lu, L., Xie, G., Jiang, Y., Du, X., and Sun, P. (2009, October) Organic vapor adsorption behavior of poly(3-henxylthiphene) films on quartz crystal microbalance. Paper presented at 2009 International Conference on Optical Instruments and Technology:Advanced Sensor Technologies and Applications. Shanghai, China.

Martin, H.P., Muller, E., Richter, R., Roewer, G., and Brendler, E. (1997) Conversion process of chlorine containing polysilanes into silicon carbide: Part I Synthesis and crosslinking of poly(chloromethyl)silanes–carbosilanes and their transformation into inorganic amorphous silicon carbide. Journal of Materials Science. 32(5), 1381-1387.

National Oceanic and Atmospheric Administration. U.D.o.C., US goverment. "Immediately Dangerous to Life and Health Limits (IDLHs)." 6 Nov 2012. 7 Nov 2012 <http://response.restoration.noaa.gov/idlhs>

Orlov, A., Ozkan, S., and Karpacheva, G. (2006) Oxidative polymerization of diphenylamine: A mechanistic study. Polymer Science Series B, 48(1), 11-17.

Penza, M. and Cassano, G. (2003) Application of principal component analysis and artificial neural networks to recognize the individual VOCs of methanol/2-propanol in a binary mixture by SAW multi-sensor array. Sensors and Actuators B: Chemical, 89(3), 269-284.

Rodríguez Presa, M.J., Posadas, D., and Florit, M.I. (2007) Conditioning treatment to improve the potentiometric pH response of polydiphenylamine modified electrodes. Sensors and Actuators B: Chemical, 123(1), 142-147.

Santhosh, P., Manesh, K.M., Gopalan, A., and Lee, K.P. (2007) Novel amperometric carbon monoxide sensor based on multi-wall carbon nanotubes grafted with polydiphenylamine—Fabrication and performance. Sensors and Actuators B: Chemical, 125(1), 92-99.

Santhosh, P., Manesh, K.M., Uthayakumar, S., Gopalan, A.I., and Lee, K.P. (2009) Hollow spherical nanostructured polydiphenylamine for direct electrochemistry and glucose biosensor. Biosensors and Bioelectronics, 24(7), 2008-2014.

Satcher, D. "Immediately Dangerous To Life or Health (IDLH)." May 1994. 31 March 2013<http://www.cdc.gov/niosh/idlh/intridl4.html>

Sathiyanarayanan, S., Muthukrishnan, S., and Venkatachari, G. (2006) Synthesis and anticorrosion properties of polydiphenylamine blended vinyl coatings. Synthetic Metals, 156(18–20), 1208-1212.

Sidebottom, H. and Franklin, J. (1996) The atmospheric fate and impact of hydrochlorofluorocarbons and chlorinated solvents. Pure and Applied Chemistry, 68(9), 1757-1769.

Silverstein, R.M., Webster, F.X., and Kiemle, D. (2005) Spectrometric Identification of Organic Compounds. New York: John Willey.

Smallwood, I.M. (1996) Handbook of Organic Solvent Properties. New York: John Willey.

Thuwachaowsoan, K., Chotpattananont, D., Sirivat, A., Rujiravanit, R., and Schwank, J.W. (2007) Electrical conductivity responses and interactions of

poly(3-thiopheneacetic acid)/zeolites L, mordenite, beta and H_2. Materials Science and Engineering: B, 140(1–2), 23-30.

Tukker, A. and Simons, Ir.L.Ph. (1999) Methylene chloride: advantages and drawbacks of possible market restrictions in the EU. Report, DG III of the European Commission, Brussels, Belgium.

Vivekanandan, J., Ponnusamy, V., Mahudeswaran, A., and Vijayanand, P.S. (2011) Synthesis, characterization and conductivity study of polyaniline prepared by chemical oxidative and electrochemical methods. Archives of Applied Science Research, 3(6), 147-153.

Whitaker, A.M. and Jones, C.S. (1965) Report of 1500 chloroform anesthetics administered with a precision vaporizer. Anesthesia & Analgesia, 44(1), 60-65.

Williams, P.L., James, R.C., and Roberts, S.M. (2000) Principles of Toxicology: Environmental and Industrial Applications. New York: John Willey.

Wu, J.Y., Liu, Q.L., Xiong, Y., Zhu, A.M., and Chen, Y. (2009) Molecular simulation of water/alcohol mixtures' adsorption and diffusion in zeolite 4A membranes. The Journal of Physical Chemistry B, 113(13), 4267-4274.

Xu, L., Hu, X., Tze Lim, Y., and Subramanian, V.S. (2002) Organic vapor adsorption behavior of poly(3-butoxythiophene) LB films on quartz crystal microbalance. Thin Solid Films, 417(1–2), 90-94.

Xu, X., Wang, J., and Long, Y. (2006) Zeolite-based materials for gas sensors. Sensors, 6(12), 1751-1764.
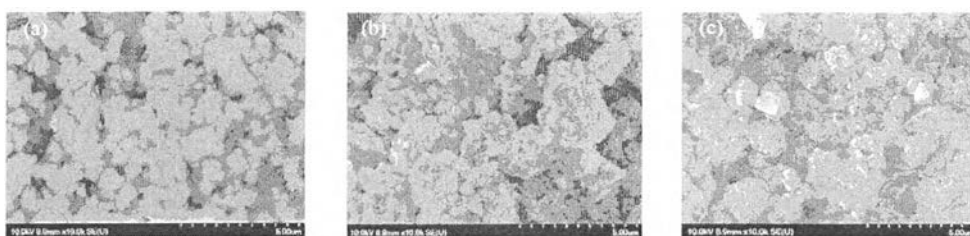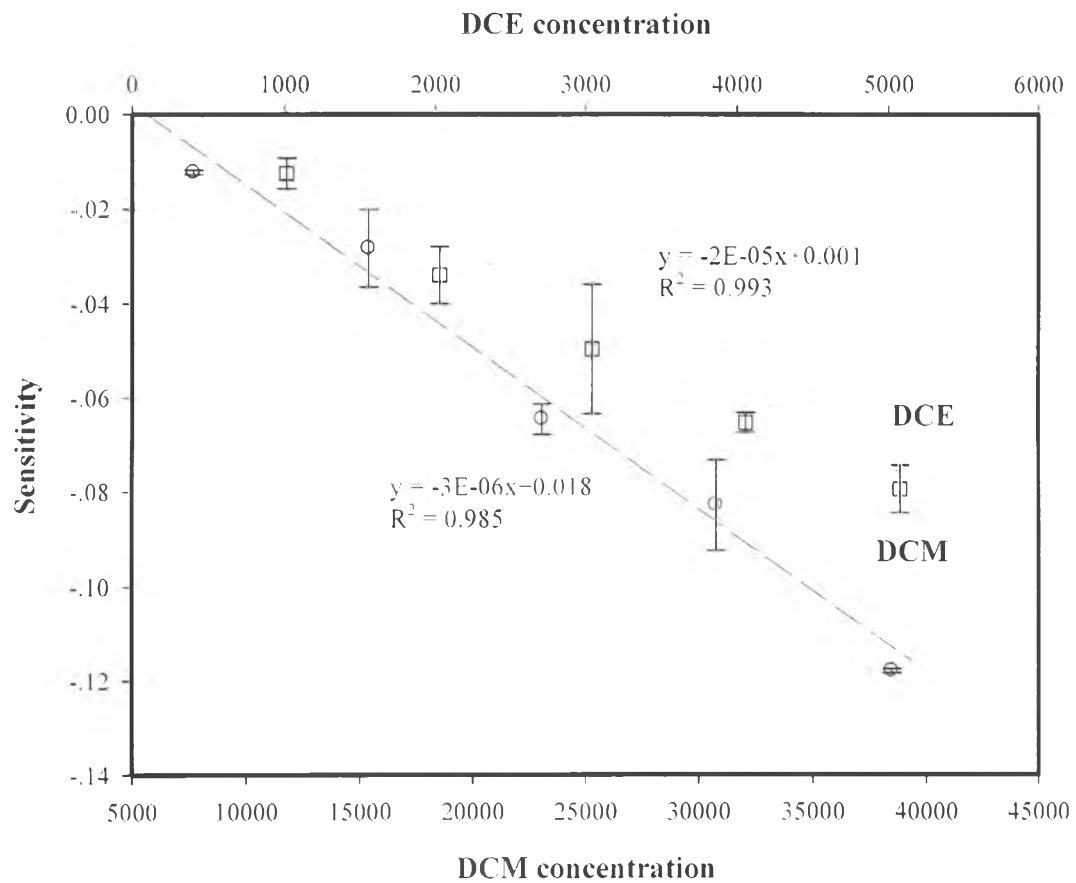
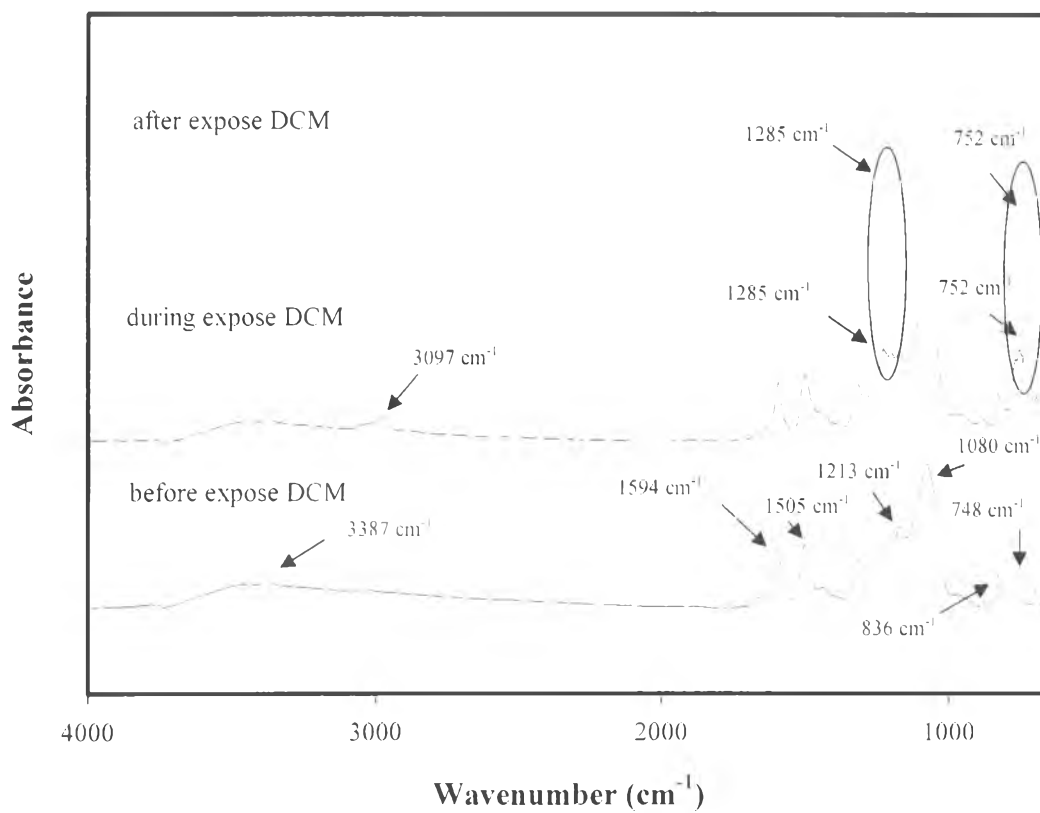**Figure 3.1** SEM micrographs at 10000x of: (a) YH: (b) D-PDPA: and (c) D-PDPA/YH.
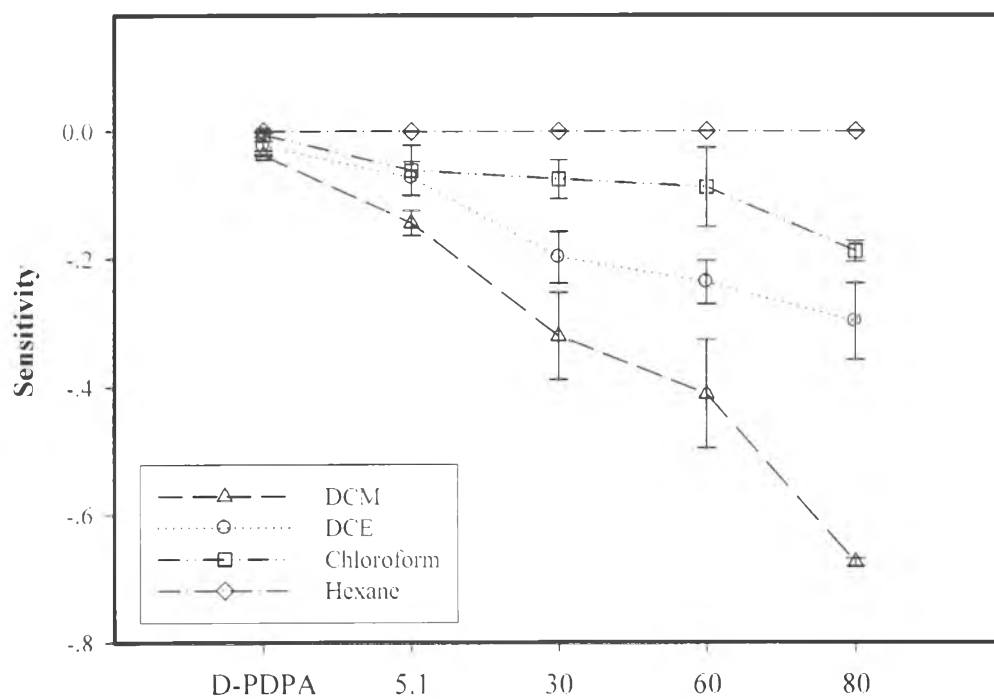
Figure 3.2 The sensitivity of D-PDPA, YH at various Si/Al ratios when exposed to halogenated solvents at 27 ± 1 °C and 1 atm.
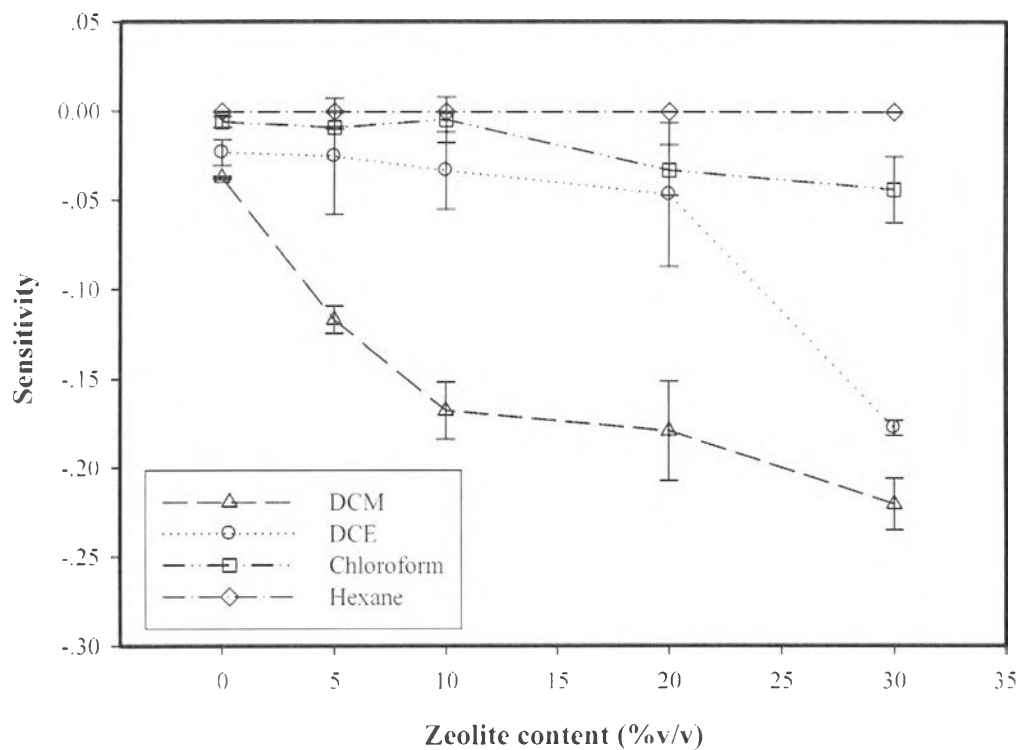
Figure 3.3 The sensitivity of D-PDPA/YH[80] at various zeolite concentrations when exposed to halogenated solvents at 27 ± 1 °C and 1 atm.
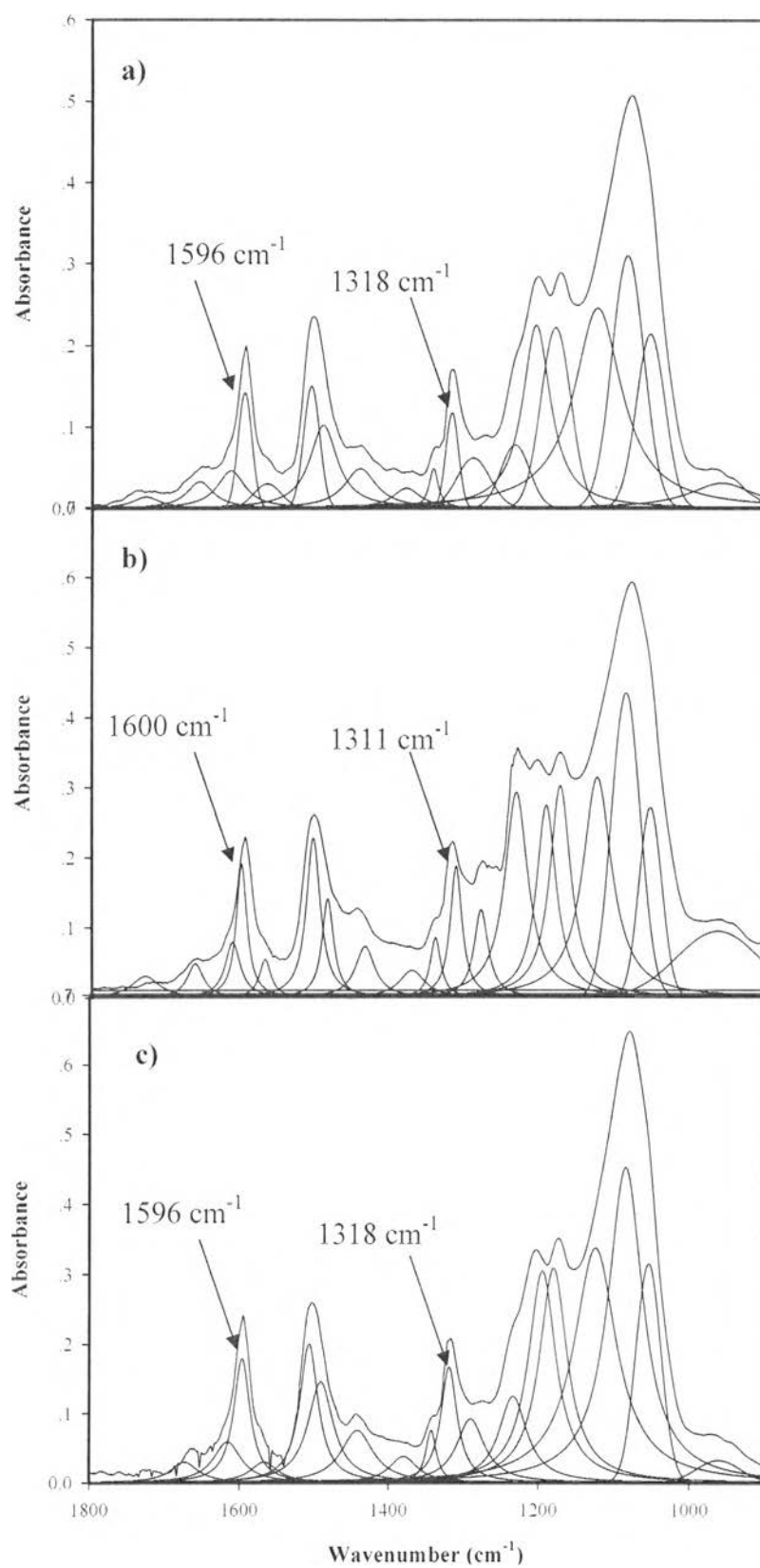
DCE concentration

Figure 3.4 The sensitivity of D-PDPA/30%YH[80] toward DCM and DCE at different concentrations at 27 ± 1 °C and 1 atm.

after expose DCM

during expose DCM

before expose DCM

Absorbance

1285 cm⁻¹

752 cm⁻¹

1285 cm⁻¹

752 cm⁻¹

3097 cm⁻¹

1080 cm⁻¹

1213 cm⁻¹

1594 cm⁻¹

1505 cm⁻¹

748 cm⁻¹

3387 cm⁻¹
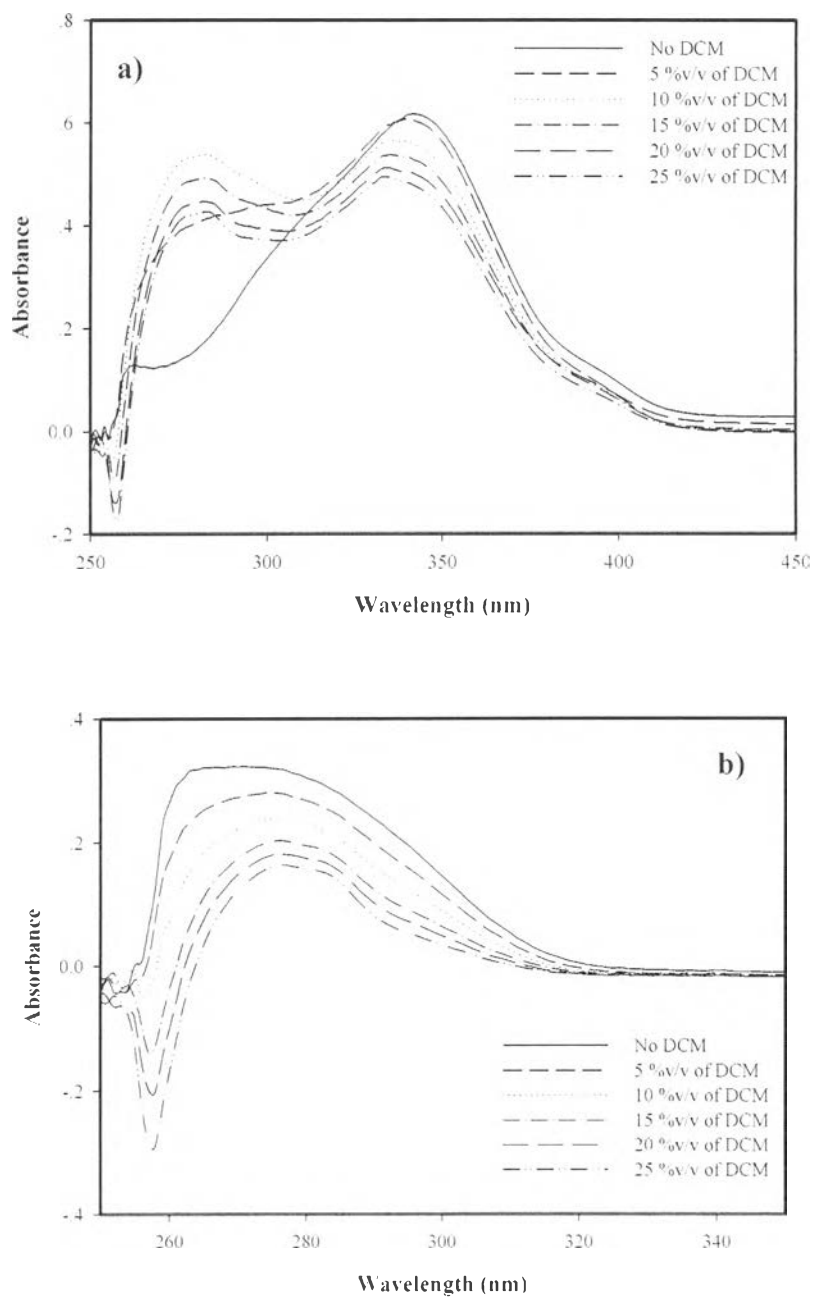
836 cm⁻¹

4000   3000   2000   1000

Wavenumber (cm⁻¹)

Figure 3.5 FT-IR spectra of D-PDPA/30% YH[80] when exposed to DCM and. DCE vapors at 27 ± 1 °C and 1 atm.
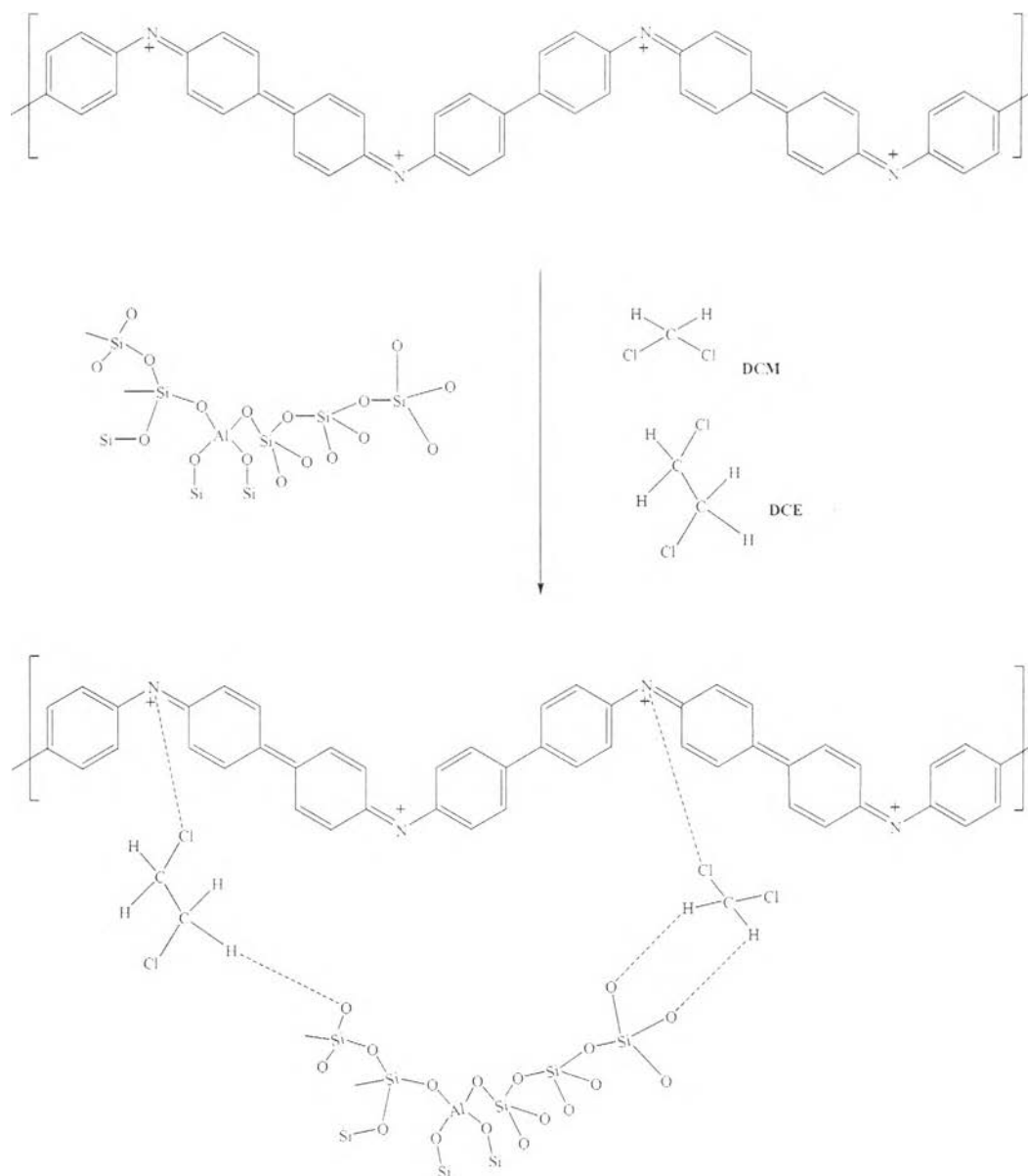
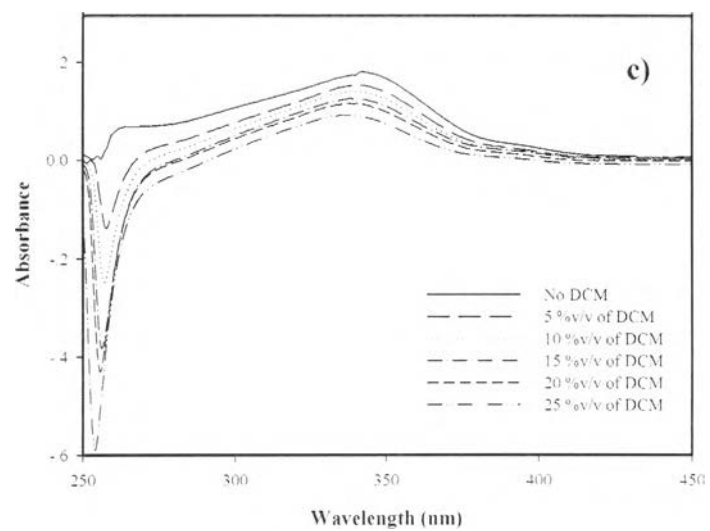**Figure 3.6** Proposed mechanism of adsorbed DCM. and DCE on D-PDPA/30% YH[80].

Figure 3.7 FT-IR second derivative of D-PDPA/30%YH[80] composite when: a) before: b) during, c) after exposed to DCM.

Figure 3.8 UV-Vis spectra of: a) D-PDPA: b) YH when exposed to DCM; and c) D-PDPA/30%YH[80] composite at various concentrations.

Figure 3.8 UV-Vis spectra of: a) D-PDPA: b) YH when exposed to DCM; and c) D-PDPA/30%YH[80] composite at various concentrations (cont.).

Table 3.1 Physical characteristics of YH

Si/Al ratio	Surface area (m^2/g)	Pore size (Å)	Pore volume (cm^3/g)
5.1	617.3 ± 2.27	3.665 ± 0.01	0.403 ± 0.01
30	731.0 ± 2.42	3.670 ± 0.02	0.569 ± 0.01
60	688.8 ± 7.62	3.675 ± 0.04	0.608 ± 0.03
80	766.1 ± 3.25	3.691 ± 0.01	0.555 ± 0.08

Table 3.2 The initial electrical conductivity of D-PDPA, YH, D-PDPA/YH[80] in N_2 before exposed to halogenated solvents at 27 ± 1 °C and 1 atm

Solvent Vapor	Initial conductivity in N_2 before exposed to the solvents, σ_{N2} (S/cm)				
	D-PDPA	YH[5.1]	YH[30]	YH[60]	YH[80]
DCM	$(2.29\pm0.91)\times10^{-4}$	$(6.49\pm2.46)\times10^{-5}$	$(7.87\pm3.45)\times10^{-5}$	$(1.31\pm0.26)\times10^{-4}$	$(2.64\pm0.39)\times10^{-4}$
DCE	$(1.83\pm0.45)\times10^{-4}$	$(6.41\pm0.76)\times10^{-5}$	$(6.98\pm0.66)\times10^{-5}$	$(7.49\pm1.63)\times10^{-5}$	$(9.34\pm1.05)\times10^{-5}$
Chloroform	$(1.34\pm0.01)\times10^{-4}$	$(9.69\pm1.15)\times10^{-5}$	$(8.92\pm0.39)\times10^{-5}$	$(9.26\pm0.05)\times10^{-5}$	$(1.44\pm0.68)\times10^{-4}$
Hexane	$(1.42\pm0.16)\times10^{-4}$	$(6.86\pm0.03)\times10^{-5}$	$(8.66\pm0.81)\times10^{-5}$	$(1.04\pm0.06)\times10^{-4}$	$(1.75\pm0.02)\times10^{-4}$
Solvent Vapor	Initial conductivity in N_2 before exposed to the solvents, σ_{N2} (Scm)				
	D-PDPA/5% YH[80]	D-PDPA/10% YH[80]	D-PDPA/20% YH[80]	D-PDPA/30% YH[80]	
DCM	$(1.60\pm0.35)\times10^{-4}$	$(1.39\pm0.07)\times10^{-4}$	$(1.97\pm0.22)\times10^{-4}$	$(2.24\pm0.04)\times10^{-4}$	
DCE	$(2.15\pm0.31)\times10^{-4}$	$(2.26\pm0.24)\times10^{-4}$	$(1.95\pm0.25)\times10^{-4}$	$(1.90\pm0.10)\times10^{-4}$	
Chloroform	$(1.70\pm0.01)\times10^{-4}$	$(1.75\pm0.14)\times10^{-4}$	$(3.08\pm1.88)\times10^{-4}$	$(2.11\pm1.03)\times10^{-4}$	
Hexane	$(1.61\pm0.02)\times10^{-4}$	$(1.41\pm0.15)\times10^{-4}$	$(1.73\pm0.07)\times10^{-4}$	$(1.34\pm0.29)\times10^{-4}$	

Table 3.3 Electrical conductivity sensitivity of D-PDPA, YH, D-PDPA/YH[80] when exposed to halogenated and non-halogenated solvents at 27 ± 1 °C and 1 atm

Material	Response ($\Delta\sigma = \sigma_{halogenated\ solvent} - \sigma_{N2}$)			
	DCM	DCE	chlroform	hexane
D-PDPA	$(-8.77\pm3.82)\times10^{-6}$	$(-1.79\pm0.73)\times10^{-5}$	$(-8.07\pm4.05)\times10^{-7}$	$(-5.11\pm3.25)\times10^{-8}$
YH[5.1]	$(-9.60\pm4.81)\times10^{-6}$	$(-4.81\pm2.25)\times10^{-6}$	$(-5.76\pm3.09)\times10^{-6}$	$(-4.30\pm0.56)\times10^{-8}$
YH[30]	$(-2.10\pm2.41)\times10^{-5}$	$(-1.32\pm0.52)\times10^{-5}$	$(-6.80\pm3.01)\times10^{-6}$	$(-5.75\pm2.70)\times10^{-8}$
YH[60]	$(-5.28\pm0.03)\times10^{-5}$	$(-1.78\pm0.09)\times10^{-5}$	$(-8.20\pm5.77)\times10^{-6}$	$(-6.61\pm2.27)\times10^{-8}$
YH[80]	$(-1.78\pm0.25)\times10^{-4}$	$(-2.39\pm1.48)\times10^{-5}$	$(-3.74\pm2.87)\times10^{-5}$	$(-1.35\pm0.35)\times10^{-7}$
D-PDPA/5% YH[80]	$(-1.86\pm0.28)\times10^{-5}$	$(-5.96\pm7.78)\times10^{-6}$	$(-1.58\pm0.02)\times10^{-6}$	$(-5.94\pm5.92)\times10^{-8}$
D-PDPA/10% YH[80]	$(-2.32\pm0.11)\times10^{-5}$	$(-7.83\pm5.74)\times10^{-6}$	$(-9.36\pm2.31)\times10^{-7}$	$(-4.86\pm0.88)\times10^{-8}$
D-PDPA/20% YH[80]	$(-3.63\pm2.35)\times10^{-5}$	$(-9.66\pm9.04)\times10^{-6}$	$(-8.90\pm1.84)\times10^{-6}$	$(-6.07\pm2.91)\times10^{-8}$
D-PDPA/30% YH[80]	$(-7.78\pm3.79)\times10^{-5}$	$(-3.37\pm0.26)\times10^{-5}$	$(-8.32\pm0.62)\times10^{-6}$	$(-5.10\pm0.50)\times10^{-8}$

Table 3.3 Electrical conductivity sensitivity of D-PDPA, YH, D-PDPA/YH[80] when exposed to halogenated and non-halogenated solvents at 27 ± 1 °C and 1 atm (cont.)

Material	Sensitivity ($\Delta\sigma/\sigma_{N2}$)			
	DCM	DCE	chlroform	hexane
D-PDPA	$(-3.83\pm0.15)\times10^{-2}$	$(-2.42\pm0.73)\times10^{-2}$	$(-6.01\pm3.02)\times10^{-3}$	$(-3.60\pm2.70)\times10^{-4}$
YH[5.1]	$(-1.48\pm0.19)\times10^{-1}$	$(-7.50\pm2.64)\times10^{-2}$	$(-5.94\pm3.92)\times10^{-2}$	$(-6.27\pm0.79)\times10^{-4}$
YH[30]	$(-2.67\pm2.09)\times10^{-1}$	$(-1.89\pm0.06)\times10^{-1}$	$(-7.63\pm3.04)\times10^{-2}$	$(-6.63\pm2.50)\times10^{-4}$
YH[60]	$(-4.03\pm0.84)\times10^{-1}$	$(-2.34\pm0.03)\times10^{-1}$	$(-8.86\pm6.18)\times10^{-2}$	$(-6.35\pm2.54)\times10^{-4}$
YH[80]	$(-6.74\pm0.06)\times10^{-1}$	$(-2.56\pm1.30)\times10^{-1}$	$(-2.60\pm0.87)\times10^{-1}$	$(-7.76\pm1.90)\times10^{-4}$
D-PDPA/5% YH[80]	$(-1.16\pm0.08)\times10^{-1}$	$(-2.90\pm0.03)\times10^{-2}$	$(-9.27\pm0.77)\times10^{-3}$	$(-3.69\pm3.68)\times10^{-4}$
D-PDPA/10% YH[80]	$(-1.67\pm0.16)\times10^{-1}$	$(-3.50\pm0.03)\times10^{-2}$	$(-5.36\pm1.28)\times10^{-3}$	$(-3.44\pm0.99)\times10^{-4}$
D-PDPA/20% YH[80]	$(-1.85\pm0.99)\times10^{-1}$	$(-5.00\pm4.03)\times10^{-2}$	$(-2.89\pm1.43)\times10^{-2}$	$(-3.51\pm0.25)\times10^{-4}$
D-PDPA/30% YH[80]	$(-3.48\pm1.64)\times10^{-1}$	$(-1.77\pm0.04)\times10^{-1}$	$(-3.95\pm1.86)\times10^{-2}$	$(-3.79\pm0.44)\times10^{-4}$

Table 3.4 Values of dielectric constant (ε), dipole moment (μ) of the solvent tested (Archer *et al.*, 2004)

Solvents	Dipole moment	Dielectric constant
Dichloromethane	1.80	9.10
1,2 dichloroethane	1.60	10.45
chloroform	1.10	4.80
hexane	0.00	1.88